IEEE Control Systems Letters paper presented at
2023 American Control Conference (ACC)
San Diego, CA, USA. May 31 - June 2, 2023

# Future-Focused Control Barrier Functions for Autonomous Vehicle Control

Mitchell Black[1] Mrdjan Jankovic[2] Abhishek Sharma[2] Dimitra Panagou[3]

*Abstract*— **In this paper, we introduce a class of future-focused control barrier functions (ff-CBF) aimed at improving traditionally myopic CBF based control design and study their efficacy in the context of an unsignaled four-way intersection crossing problem for collections of both communicating and non-communicating autonomous vehicles. Our novel ff-CBF encodes that vehicles take control actions that avoid collisions predicted under a zero-acceleration policy over an arbitrarily long future time interval. In this sense the ff-CBF defines a virtual barrier, a loosening of which we propose in the form of a relaxed future-focused CBF (rff-CBF) that allows a relaxation of the virtual ff-CBF barrier far from the physical barrier between vehicles. We study the performance of ff-CBF and rff-CBF based controllers on communicating vehicles via a series of simulated trials of the intersection scenario, and in particular highlight how the rff-CBF based controller empirically outperforms a benchmark controller from the literature by improving intersection throughput while preserving safety and feasibility. Finally, we demonstrate our proposed ff-CBF control law on an intersection scenario in the laboratory environment with a collection of 5 non-communicating AION ground rovers.**

## I. Introduction

Vehicles with autonomous capabilities have grown increasingly prevalent on public roadways in recent years, and growth is forecasted to continue [1]. Intersection scenarios are of keen interest due to the systemic dangers they pose; in fact, according to the U.S. Federal Highway Administration more than 50% of all fatal and injury crashes occur at intersections [2]. Some have proposed alleviating this problem by using a centralized intersection manager (IM) to communicate safe entry/exit times to incoming connected autonomous vehicles (CAVs) [3]–[5]. In contrast to schedulers, controllers offer better real-time reactivity to a dynamic, evolving environment. In the intersection setting, it is critical that control solutions are designed such that the overall system possesses both safety and liveness properties, i.e. that vehicles are able to traverse the intersection safely.

In both centralized and decentralized approaches, a common element in safe controller design is the use of control barrier functions (CBFs) [6], [7]. CBFs have been shown to be effective in compensating for some potentially unsafe control action in a variety of applications, including autonomous driving [8], robotic manipulators [9], and quadrotor control [10]. Studies have further demonstrated that CBFs are useful in maintaining safety in the presence of bounded disturbances [11] and model uncertainties [12]. To date, however, a difficulty encountered when using CBF-based approaches is their tendency to myopically focus on present safety, potentially to the detriment of future performance. This drawback can be mitigated in part by using model predictive control (MPC), which solves an optimal control problem over a time horizon and implements the present control solution. While some recent work has demonstrated the efficacy of synthesizing CBFs with MPC frameworks for safe control [13], such controllers often require the solution to a sequence of optimization problems at a given time, where the size of each optimization grows with the look-ahead horizon.

Motivated by these drawbacks, we introduce a new future-focused control barrier function (ff-CBF) for collision avoidance. Its fundamental underlying assumption is that vehicles seek to minimize unnecessary acceleration (or deceleration), inspired by the widespread use of energy-efficient minimum-norm controllers [14]–[16]. This assumption is manifested as a constant velocity prediction of the positions of surrounding vehicles. We then use this to define the predicted minimum inter-agent distance over a future time interval and enforce that this distance remains above a safe threshold. In other words, the ff-CBF defines a zero super-level set containing vehicle states that are guaranteed to remain safe under a zero-acceleration (i.e. constant velocity) control policy over a period of time. It is worth noting that ff-CBFs are related to predictive CBFs, which were developed in parallel, introduced in [17], and take on an increased computational load in exchange for applicability to more general predicted trajectories. In this sense, ff-CBFs (like predictive CBFs) are related to recent work on the development of backup CBF policies [18]–[20]. Unlike backup and predictive CBF policies, however, our ff-CBF does not require numerical integration of the system trajectories forward in time, the computational demands of which also grow with the look-ahead horizon. This allows us to take predicted future safety into account for the design of present actions while using a computationally-efficient quadratic program-based control law often used for CBF-based safe control [6], [8], [9], [12].

Our future-focused CBF, however, defines a *virtual* barrier which, in practice, may be violated without defying the *physical* barrier between agents. As such, we introduce the notion of a relaxed future-focused control barrier function (rff-CBF) and show that enforcing forward invariance of its zero super-level set allows permeability of the virtual barrier while satisfying the physical one. The rff-CBF, therefore, permits

We would like to acknowledge the support of the Ford Motor Company, and of the National Science Foundation under award number 1931982.

[1]Department of Aerospace Engineering, University of Michigan, 1320 Beal Ave., Ann Arbor, MI 48109, USA; mblackjr@umich.edu.

[2]Ford Research and Advanced Engineering, 2101 Village Rd., Dearborn, MI 48124, USA; {mjankov1, asharm90}@ford.com.

[3]Dept. of Robotics and Dept. of Aerospace Engineering, Univ. of Michigan, Ann Arbor, MI 48109, USA; dpanagou@umich.edu.

the execution of safe control actions deemed inadmissible by the ff-CBF, resulting in reduced conservatism. In a numerical study, we examine the intersection crossing problem over a wide variety of initial conditions and highlight how an rff-CBF based controller provides the safety and performance benefits of ff-CBF based control while improving feasibility properties of a quadratic program (QP) based control law. We then implement the rff-CBF controller on a collection of ground rovers in a lab environment, and demonstrate its success in safely driving non-communicating vehicles through an unsignaled intersection.

The paper is organized as follows. Section II introduces some preliminaries, including set invariance and QP-based control. We formalize the problem under consideration in Section III and introduce our future-focused CBF in Section IV. Section V contains the results of our simulated and experimental trials, and in Section VI we conclude with final remarks and directions for future work.

## II. Mathematical Preliminaries

We use the following notation throughout the paper. $\mathbb{R}$ denotes the set of real numbers. $\|\cdot\|$ represents the Euclidean norm (2-norm). We use lowercase variables for scalar quantities (e.g., $a \in \mathbb{R}$), lowercase bold variables for vector quantities (e.g., $\boldsymbol{x} \in \mathbb{R}^n$), and uppercase bold variables for matrices (e.g., $\boldsymbol{M} \in \mathbb{R}^{m\times n}$). $\mathcal{C}^r$ is the set of $r$-times continuously differentiable functions in all arguments. We write $\partial\mathcal{S}$ for the boundary of a closed set $\mathcal{S}$, and $\text{Int}(\mathcal{S})$ for its interior. A function $\alpha$ is said to belong to class $\mathcal{K}_\infty$ if $\alpha(0) = 0$ and $\alpha : \mathbb{R} \to \mathbb{R}$ is increasing on the interval $(-\infty, \infty)$. The Lie derivative of a function $V : \mathbb{R}^n \to \mathbb{R}$ along a vector field $f : \mathbb{R}^n \to \mathbb{R}^n$ at a point $\boldsymbol{x} \in \mathbb{R}^n$ is denoted $L_f V(\boldsymbol{x}) \triangleq \frac{\partial V}{\partial \boldsymbol{x}} f(\boldsymbol{x})$.

In this paper, we consider a collection of agents, $\mathcal{A}$, each of whose dynamics is governed by the following class of nonlinear, control-affine systems

$$\dot{\boldsymbol{x}}_i = f_i(\boldsymbol{x}_i(t)) + g_i(\boldsymbol{x}_i(t))\boldsymbol{u}_i(t), \quad \boldsymbol{x}_i(0) = \boldsymbol{x}_{i0}, \tag{1}$$

where $\boldsymbol{x}_i \in \mathbb{R}^n$ and $\boldsymbol{u}_i \in \mathcal{U}_i \subset \mathbb{R}^m$ denote the state and control vectors respectively for agent $i \in \mathcal{A}$, and where $f_i : \mathbb{R}^n \to \mathbb{R}^n$ and $g_i : \mathbb{R}^n \to \mathbb{R}^{n\times m}$ are locally Lipschitz in their arguments and not necessarily homogeneous across agents. The set $\mathcal{U}_i$ denotes the set of admissible control inputs, and it is assumed that $\mathcal{A}$ has cardinality $p$. A subset of agents $\mathcal{A}_c \subseteq \mathcal{A}$ is assumed to be communicating in that they share information (e.g., control inputs) and thus may use centralized control laws, whereas the remaining agents $\mathcal{A}_n = \mathcal{A} \setminus \mathcal{A}_c$ are non-communicating and must resort to decentralized control laws.

Given a continuously differentiable function $h_i : \mathbb{R}^n \to \mathbb{R}$, we define a safe set $\mathcal{S}_i$ as

$$\mathcal{S}_i = \{\boldsymbol{x}_i \in \mathbb{R}^n \mid h_i(\boldsymbol{x}_i) \geq 0\}, \tag{2}$$

where the boundary and interior of $\mathcal{S}_i$ are $\partial\mathcal{S}_i = \{\boldsymbol{x}_i \in \mathbb{R}^n \mid h_i(\boldsymbol{x}_i) = 0\}$ and $\text{Int}(\mathcal{S}_i) = \{\boldsymbol{x}_i \in \mathbb{R}^n \mid h_i(\boldsymbol{x}_i) > 0\}$ respectively. The trajectories of (1) remain safe, i.e. $\boldsymbol{x}_i(t) \in \mathcal{S}_i$ for all $t \geq 0$, if $\mathcal{S}_i$ is *forward-invariant*. The following constitutes a necessary and sufficient condition for forward invariance of a set $\mathcal{S}_i$.

**Lemma 1** (Nagumo's Theorem [21])**.** *Suppose that there exists $\boldsymbol{u}_i \in \mathcal{U}_i$ such that (1) admits a globally unique solution for each $\boldsymbol{x}_i(0) \in \mathcal{S}_i$. Then, the set $\mathcal{S}_i$ is forward-invariant for the controlled system (1) if and only if*

$$L_{f_i} h_i(\boldsymbol{x_i}) + L_{g_i} h_i(\boldsymbol{x_i})\boldsymbol{u}_i \geq 0, \ \forall \boldsymbol{x}_i \in \partial\mathcal{S}_i. \tag{3}$$

One way to render a set forward-invariant is to use CBFs in the control design.

**Definition 1.** *[6, Definition 5] Given a set $\mathcal{S}_i \subset \mathbb{R}^n$ defined by (2) for a continuously differentiable function $h_i : \mathbb{R}^n \to \mathbb{R}$, the function $h_i$ is a **control barrier function** (CBF) defined on a set $\mathcal{D}_i$, where $\mathcal{S}_i \subseteq \mathcal{D}_i \subset \mathbb{R}^n$, if there exists a Lipschitz continuous function $\alpha \in \mathcal{K}_\infty$ such that, $\forall \boldsymbol{x}_i \in \mathcal{D}_i$,*

$$\sup_{\boldsymbol{u}_i \in \mathcal{U}_i} [L_{f_i} h_i(\boldsymbol{x_i}) + L_{g_i} h_i(\boldsymbol{x_i})\boldsymbol{u}_i] \geq -\alpha(h_i(\boldsymbol{x_i})). \tag{4}$$

It is evident that (4) reduces to (3) when $\boldsymbol{x}_i \in \partial\mathcal{S}_i$, thus if $h_i(\boldsymbol{x}(0)) \geq 0$ and $h_i$ is a CBF on $\mathcal{D}_i$ then $\mathcal{S}_i$ can be rendered forward-invariant. As such, it has become popular to include CBF conditions (4) as linear constraints in a quadratic program (QP) based control law [6], [8], etc. When agents in the system are cooperative and communicating, a centralized controller may be deployed as follows

$$\boldsymbol{u}^* = \underset{\boldsymbol{u}\in\mathcal{U}}{\arg\min} \frac{1}{2}\|\boldsymbol{u} - \boldsymbol{u}^0\|^2 \tag{5a}$$
$$\text{s.t.} \quad \forall i, j = 1, \ldots, p, \ i \neq j$$
$$\phi_i + \boldsymbol{\gamma}_i \boldsymbol{u}_i \geq 0, \tag{5b}$$
$$\phi_{ij} + \boldsymbol{\gamma}_{ij} \boldsymbol{u} \geq 0, \tag{5c}$$

where $\boldsymbol{u} = [\boldsymbol{u}_1, \ldots, \boldsymbol{u}_p]^\top$ and $\boldsymbol{u}^0 = [\boldsymbol{u}_1^0, \ldots, \boldsymbol{u}_p^0]^\top$ denote concatenations of the input and nominal input vectors respectively, and

$$\phi_i = L_{f_i} h_i(\boldsymbol{x}_i) + \alpha_i(h_i(\boldsymbol{x}_i)), \tag{6a}$$
$$\phi_{ij} = L_{f_i} h_{ij}(\boldsymbol{x}_i, \boldsymbol{x}_j) + L_{f_j} h_{ij}(\boldsymbol{x}_i, \boldsymbol{x}_j) + \alpha_{ij}(h_{ij}(\boldsymbol{x}_i, \boldsymbol{x}_j)), \tag{6b}$$
$$\boldsymbol{\gamma}_i = L_{g_i} h_i(\boldsymbol{x}_i), \tag{6c}$$
$$\boldsymbol{\gamma}_{ij} = [L_{g_1} h_{ij}(\boldsymbol{x}_i, \boldsymbol{x}_j) \ldots L_{g_p} h_{ij}(\boldsymbol{x}_i, \boldsymbol{x}_j)], \tag{6d}$$

where each $\alpha_i, \alpha_{ij} \in \mathcal{K}_\infty$ such that (5b) represents an agent-specific constraint (e.g., speed limit) and (5c) represents an inter-agent constraint (e.g., collision avoidance). Note that $\boldsymbol{\gamma}_{ij}$ is a row vector of all zeros except indices $i$ and $j$, denoted $\boldsymbol{\gamma}_{ij,[i]}$ and $\boldsymbol{\gamma}_{ij,[j]}$ respectively. If the agents are non-communicating, however, then a decentralized control law of the following form may be used:

$$\boldsymbol{u}_i^* = \underset{\boldsymbol{u}_i\in\mathcal{U}_i}{\arg\min} \frac{1}{2}\|\boldsymbol{u}_i - \boldsymbol{u}_i^0\|^2 \tag{7a}$$
$$\text{s.t.} \ \forall j = 1, \ldots, p, \ i \neq j$$
$$\phi_i + \boldsymbol{\gamma}_i \boldsymbol{u}_i \geq 0, \tag{7b}$$
$$\phi_{ij} + \boldsymbol{\gamma}_{ij,[i]} \boldsymbol{u}_i \geq 0, \tag{7c}$$

where (7b) and (7c) represent agent-specific and inter-agent constraints similar to (5b) and (5c). As noted by [22], collision avoidance is guaranteed under the centralized control scheme (5) whenever it is feasible, unlike the decentralized controller (7) under which (for a generic CBF $h_{ij}$) no such guarantee exists even when used uniformly by all agents. In Section V, we use forms of (5) and (7) to solve versions of the intersection crossing problem outlined in Section III.

## III. Problem Formulation

Let $\mathcal{F}$ be an inertial frame with a point $s_0$ denoting its origin. Consider a collection of vehicles $\mathcal{A}$ approaching an unsignaled four-way intersection, where the dynamics of the $i^{\text{th}}$ vehicle are modeled as

$$\dot{x}_i = v_i \left(\cos\psi_i - \sin\psi_i \tan\beta_i\right), \tag{8a}$$
$$\dot{y}_i = v_i \left(\sin\psi_i + \cos\psi_i \tan\beta_i\right), \tag{8b}$$
$$\dot{\psi}_i = \frac{v_i}{l_r}\tan\beta_i, \tag{8c}$$
$$\dot{\beta}_i = \omega_i, \tag{8d}$$
$$\dot{v}_i = a_i, \tag{8e}$$

where $x_i$ and $y_i$ denote the position of the center of gravity (c.g.) of the vehicle with respect to $s_0$, $\psi_i$ is the orientation of the body-fixed frame, $\mathcal{B}_i$, with respect to $\mathcal{F}$, $\beta_i$ is the slip angle[1] of the vehicle c.g. relative to $\mathcal{B}_i$ (we assume $|\beta_i| < \frac{\pi}{2}$), and $v_i$ is the velocity of the rear wheel with respect to $\mathcal{F}$. The state of vehicle $i$ is denoted by $\boldsymbol{z}_i = [x_i\ y_i\ \psi_i\ \beta_i\ v_i]^\top$, and the full state is $\boldsymbol{z} = [\boldsymbol{z}_1 \dots \boldsymbol{z}_p]^\top$. The control input is $\boldsymbol{u}_i = [\omega_i\ a_i]^\top$, where $a_i$ is the linear acceleration of the rear wheel and $\omega_i$ the angular velocity of the slip angle, $\beta_i$, which is related to the steering angle, $\delta_i$, via $\tan\beta_i = \frac{l_r}{l_r+l_f}\tan\delta_i$, where $l_f + l_r$ is the wheelbase with $l_f$ (resp. $l_r$) the distance from the c.g. to the center of the front (resp. rear) wheel. The model, depicted in Figure 1, is a dynamic extension of the kinematic bicycle model described in [23, Chapter 2], and is often used for autonomous vehicles [24].

For safety, we consider that each vehicle must 1) obey the road speed limit and drive only in the forward direction, 2) remain inside the road boundaries, and 3) avoid collisions with all vehicles. The satisfaction of requirement 2) can be handled via nominal design of $\omega_i$, whereas we encode 1) and 3) with the following candidate CBFs:

$$h_{s,i}(\boldsymbol{z}_i) = (v_{max} - v_{r,i})(v_{r,i}), \tag{9}$$
$$h_{0,ij}(\boldsymbol{z}_i, \boldsymbol{z}_j) = (x_i - x_j)^2 + (y_i - y_j)^2 - (2R)^2, \tag{10}$$

where $v_{max}$ denotes the speed limit in m/s and $R$ is a safe radius in m. We note that (10) is widely used in the literature to encode collision avoidance [22], [25]. Thus, $h_{s,i}$ and $h_{0,ij}$ define the following safe sets at time $t$: $\mathcal{S}_{s,i}(t) = \{\boldsymbol{z}_i(t) : h_{s,i}(\boldsymbol{z}_i(t)) \geq 0\}$ and $\mathcal{S}_{0,ij}(t) = \{(\boldsymbol{z}_i(t), \boldsymbol{z}_j(t)) : h_{0,ij}(\boldsymbol{z}_i(t), \boldsymbol{z}_j(t)) \geq 0\}$, the intersection of which constitutes the safe set for a given vehicle, i.e.

$$\mathcal{S}_i(t) = \{\mathcal{S}_{s,i}(t) \cap \mathcal{S}_{0,i}(t)\}, \tag{11}$$

[1]The slip angle is the angle between the velocity vector associated with a point in a frame and the orientation of the frame.

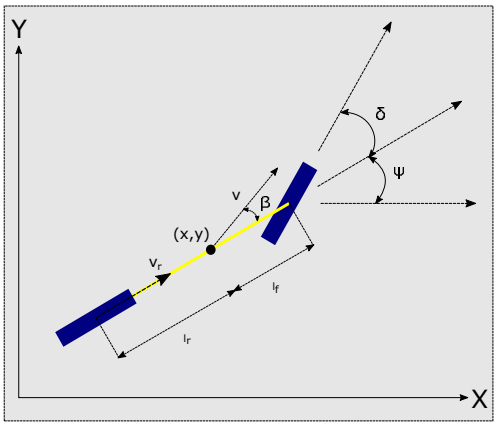


Fig. 1: Diagram of bicycle model described in (8).

where $\mathcal{S}_{0,i}(t) = \bigcap_{j=1, j\neq i}^{N} \mathcal{S}_{0,ij}(t)$.

Before introducing the problem under consideration, we note that the dynamics (8) under some predicted control policy $\hat{\boldsymbol{u}}_i$ may be expressed as

$$\dot{\hat{\boldsymbol{z}}}_i = f_i(\hat{\boldsymbol{z}}_i(t)) + g_i(\hat{\boldsymbol{z}}_i(t))\hat{\boldsymbol{u}}_i,\ \hat{\boldsymbol{z}}_i(t_0) = \boldsymbol{z}_i(t_0), \tag{12}$$

where $\hat{\boldsymbol{z}}_i \in \mathbb{R}^n$ denotes the state predicted under the policy $\hat{\boldsymbol{u}}_i$. At any time instance, the predicted dynamics (12) may be propagated forward in time to determine a state prediction at some future time $\tau > t_0$. In this paper, we take $\hat{\boldsymbol{u}}_i$ to be the zero-acceleration policy, defined as $\hat{\boldsymbol{u}}_i \triangleq [\hat{\omega}_i\ \hat{a}_i]^\top = [0\ 0]^\top$.

**Assumption 1.** *Let $0 < \bar{\tau} < \infty$. For all vehicles $i \in \mathcal{A}$ with dynamics governed by (8), assume that the predicted closed-loop trajectories of (12) under the zero-acceleration policy $\hat{\boldsymbol{u}}_i$ beginning at $t_0 = 0$ are safe over the interval $\tau \in [0, \bar{\tau}]$, i.e. $\hat{\boldsymbol{z}}_i(\tau) \in \mathcal{S}_i(\tau)$ for all $\tau \in [0, \bar{\tau}]$, $\forall i \in \mathcal{A}$.*

Assumption 1 states that no collisions shall occur between vehicles traveling with constant velocity within a time $\bar{\tau}$ of the initial time instant, i.e. no vehicles are on a collision course at the outset.

**Problem 1.** *Consider a set of vehicles ($i \in \mathcal{A}$) whose dynamics are described by (8). Given Assumption 1, design a control law, $\boldsymbol{u}_i^*(t) = [\omega_i^*(t)\ a_i^*(t)]^\top$, such that, $\forall i \in \mathcal{A}$,*

*i) the closed-loop trajectories of (8) remain safe for all time ($\boldsymbol{z}_i(t) \in \mathcal{S}_i(t)$, $\forall t \geq 0$), and*

*ii) at every time $t \geq 0$ the predicted closed-loop trajectories of (12) over the interval $\tau \in [t, t+\bar{\tau}]$ remain safe under the zero-acceleration policy $\hat{\boldsymbol{u}}_i$, i.e. $\hat{\boldsymbol{z}}_i(\tau) \in \mathcal{S}_i(\tau)$, $\forall \tau \in [t, t+\bar{\tau}]$, $\forall t \geq 0$ under $\hat{\boldsymbol{u}}_i(\tau)$.*

The look-ahead time $\bar{\tau}$ directly influences the set of allowable initial conditions, and vice versa: given $\bar{\tau}$, the set of allowable initial conditions is restricted to $\mathcal{Z}_0(\bar{\tau}) = \{\boldsymbol{z} \in \mathbb{R}^{pn} : F(\boldsymbol{z}, \bar{\tau}) \geq 0\}$, where $F : \mathbb{R}^{pn} \times \mathbb{R}_{\geq 0} \to \mathbb{R}$ is negative if vehicles are predicted to collide under $\hat{\boldsymbol{u}}_i$ and non-negative otherwise. On the other hand, given the set of initial states $\mathcal{Z}_0$, the allowable values of $\bar{\tau}$ are those for which no collisions occur under $\hat{\boldsymbol{u}}_i$ over the initial time interval $[0, \bar{\tau}]$.

In the following section, we introduce a function that serves as a facet of our proposed solution to Problem 1: a future-focused control barrier function (ff-CBF) suitable for QP-based controllers.

## IV. Future-Focused Control Barrier Functions

We first recall the nominal CBF for inter-agent safety (10), and note that for two agents $i$ and $j$ it may be rewritten as

$$h_{0,ij}(\boldsymbol{z}_i, \boldsymbol{z}_j) = D_{ij}^2(\boldsymbol{z}_i, \boldsymbol{z}_j) - (2R)^2, \tag{13}$$

where $D_{ij}(\boldsymbol{z}_i, \boldsymbol{z}_j) = \sqrt{(x_i - x_j)^2 + (y_i - y_j)^2}$. Let the differential inter-agent position, $\boldsymbol{\xi}_{ij}$, velocity, $\boldsymbol{\nu}_{ij}$, and acceleration, $\boldsymbol{\alpha}_{ij}$, vectors be

$$\begin{aligned}
\boldsymbol{\xi}_{ij} &= [\xi_{x,ij},\ \xi_{y,ij}]^\top = [x_i - x_j,\ y_i - y_j]^\top, \\
\boldsymbol{\nu}_{ij} &= [\nu_{x,ij},\ \nu_{y,ij}]^\top = [\dot{x}_i - \dot{x}_j,\ \dot{y}_i - \dot{y}_j]^\top, \\
\boldsymbol{\alpha}_{ij} &= [\alpha_{x,ij},\ \alpha_{y,ij}]^\top = [\ddot{x}_i - \ddot{x}_j,\ \ddot{y}_i - \ddot{y}_j]^\top,
\end{aligned}$$

where we have omitted the argument $t$ for conciseness. In what follows, we also drop the subscript $ij$ from $D$, $\xi$, $\nu$, and $\alpha$. The critical observation is that the inter-agent distance at any arbitrary time, $T$, is $D(\boldsymbol{z}_i, \boldsymbol{z}_j, T) = \|\boldsymbol{\xi}(T)\|$. By assuming zero acceleration, we can use a linear model to predict that at time $T = t + \tau$, we will have that $\boldsymbol{\xi}(t + \tau) = \boldsymbol{\xi}(t) + \boldsymbol{\nu}(t)\tau$, which implies that the predicted distance at a time of $t + \tau$ is

$$D(\boldsymbol{z}_i, \boldsymbol{z}_j, t + \tau) = \sqrt{\xi_x^2 + \xi_y^2 + 2\tau(\xi_x\nu_x + \xi_y\nu_y) + \tau^2(\nu_x^2 + \nu_y^2)}.$$

Then, we may define the minimum predicted future distance between agents under the zero-acceleration policy as

$$D(\boldsymbol{z}_i, \boldsymbol{z}_j, t + \tau^*) = \|\boldsymbol{\xi}(t) + \boldsymbol{\nu}(t)\tau^*\|, \tag{14}$$

where

$$\tau^* = \arg\min_{\tau \in \mathbb{R}} D^2(\boldsymbol{z}_i, \boldsymbol{z}_j, t + \tau) = -\frac{\xi_x\nu_x + \xi_y\nu_y}{\nu_x^2 + \nu_y^2}. \tag{15}$$

We elect to consider the zero-acceleration policy, however, due to the resulting mathematical simplicity (no forward integration required) and the popularity of minimum-norm controllers (e.g., [15], [16]) seeking the smallest admissible acceleration.

We now introduce our future-focused CBF for collision avoidance, the effect of which is depicted in Figure 2:

$$h_{\hat{\tau},ij}(\boldsymbol{z}_i, \boldsymbol{z}_j) = D_{ij}^2(\boldsymbol{z}_i, \boldsymbol{z}_j, t + \hat{\tau}) - (2R)^2, \tag{16}$$

where

$$\hat{\tau} = \hat{\tau}^* K_0(\hat{\tau}^*) + (\bar{\tau} - \hat{\tau}^*)K_{\bar{\tau}}(\hat{\tau}^*), \tag{17}$$

with $\bar{\tau} > 0$ representing the length of the look-ahead horizon, $K_\delta(s) = \frac{1}{2} + \frac{1}{2}\tanh(k(s - \delta))$, $k > 0$, and

$$\hat{\tau}^* = -\frac{\xi_x\nu_x + \xi_y\nu_y}{\nu_x^2 + \nu_y^2 + \varepsilon}, \tag{18}$$

where $0 < \varepsilon \ll 1$. Using (17) alleviates undesirable characteristics of (15), namely that $\tau^*$ may become unbounded. The inclusion of $\varepsilon$ makes (18) well-defined, and $K_\delta(t)$ allows (17) to smoothly approximate $\hat{\tau}^*$ between 0 and $\bar{\tau}$.

It is worth mentioning that the ff-CBF is related to the backup CBFs used for safe control design in [18], [19] in the following sense: whereas past works have required a backup policy to actively intervene to preserve safety (e.g., by applying proportional braking, see [22]), our formulation encodes that present control actions prevent future unsafe scenarios that *would* occur if all vehicles employed a zero-acceleration policy. Thus, the ff-CBF seeks to preserve the viability of the zero-acceleration policy as a safe backup policy.

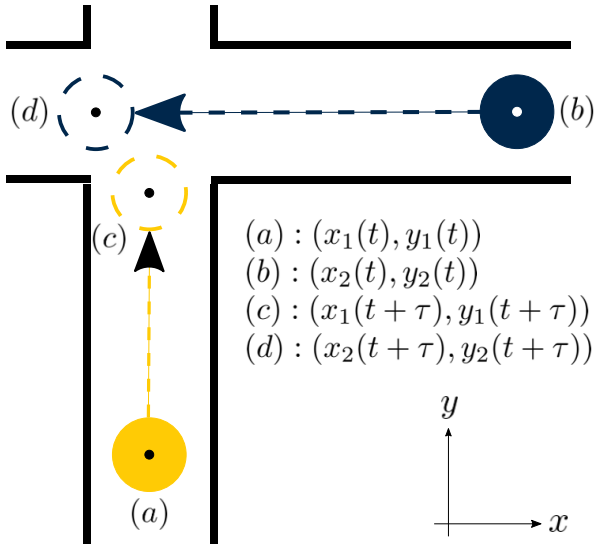


Fig. 2: Visualization of the effect of the ff-CBF. Whereas $h_{0,12}$ is evaluated based on the locations of vehicles 1 and 2 at time $t$, i.e. $(a)$ and $(b)$, $h_{\tau,12}$ judges safety based on the predicted future locations of the vehicles at time $t + \tau$, i.e. $(c)$ and $(d)$, allowing the present control to take action to avoid predicted future danger.

**Theorem 1.** *Consider two agents governed by the dynamics (8) whose states are $\boldsymbol{z}_i$ and $\boldsymbol{z}_j$. Suppose that $h_{\hat{\tau},ij}$ is defined by (16), with $\hat{\tau}$ given by (17). Then, the following hold for all bounded $\boldsymbol{z}_i$, $\boldsymbol{z}_j$:*

*i)* $h_{\hat{\tau},ij} \in \mathcal{C}^1$

*ii)* $h_{\hat{\tau},ij} \leq h_{0,ij}$ *whenever* $\hat{\tau} \leq 2\hat{\tau}^*$

*Proof.* For the first part, we must show that the derivative of (16) is well-defined and continuous. Consider that from (14), (16), and (17) we have

$$\begin{aligned}
\dot{h}_{\hat{\tau},ij}(\boldsymbol{z}) = {} & 2\xi_x\nu_x + 2\xi_y\nu_y + 2\dot{\hat{\tau}}(\xi_x\nu_x + \xi_y\nu_y) \\
& + 2\hat{\tau}(\nu_x^2 + \nu_y^2 + \xi_x\alpha_x + \xi_y\alpha_y) \\
& + 2\hat{\tau}\dot{\hat{\tau}}(\nu_x^2 + \nu_y^2) + 2\hat{\tau}^2(\nu_x\alpha_x + \nu_y\alpha_y).
\end{aligned} \tag{19}$$

Since $\hat{\tau}$ is bounded by definition, it follows that $h_{\hat{\tau},ij} \in \mathcal{C}^1$ when $\hat{\tau} \in \mathcal{C}^1$. From (17), we have

$$\dot{\hat{\tau}} = \dot{\hat{\tau}}^*\left(K_0(\hat{\tau}^*) - K_{\bar{\tau}}(\hat{\tau}^*)\right) + \hat{\tau}^*\left(\dot{K}_0(\hat{\tau}^*) - \dot{K}_{\bar{\tau}}(\hat{\tau}^*)\right) + \bar{\tau}\dot{K}_{\bar{\tau}}(\hat{\tau}^*),$$

where

$$\dot{K}_\delta(\hat{\tau}^*) = \dot{\hat{\tau}}^*\frac{k}{2}\operatorname{sech}^2\left(k(\hat{\tau}^* - \delta)\right)$$

and from (18)

$$\dot{\hat{\tau}}^* = -\frac{\alpha_x(2\nu_x\tau^* + \xi_x) + \alpha_y(2\nu_y\tau^* + \xi_y) + \nu_x^2 + \nu_y^2}{\nu_x^2 + \nu_y^2 + \varepsilon}$$

since $\dot{\hat{\tau}}^*$ and $\dot{K}_\delta(t)$ are bounded and continuous for bounded arguments, we have that $\hat{\tau} \in \mathcal{C}^1$ for bounded $\boldsymbol{z}_i$, $\boldsymbol{z}_j$. Thus, $h_{\hat{\tau},ij} \in \mathcal{C}^1$.

For the second part, we observe that $h_{\hat{\tau},ij}(\boldsymbol{z}) = h_{0,ij}(\boldsymbol{z}) + 2\hat{\tau}(\xi_x\nu_x + \xi_y\nu_y) + \hat{\tau}^2(\nu_x^2 + \nu_y^2)$, thus $h_{\hat{\tau},ij}(\boldsymbol{z}_i, \boldsymbol{z}_j) \leq h_{0,ij}(\boldsymbol{z}_i, \boldsymbol{z}_j)$ whenever

$$\hat{\tau} \leq -2\frac{\xi_x\nu_x + \xi_y\nu_y}{\nu_x^2 + \nu_y^2} = 2\tau^*. \tag{20}$$

With $\varepsilon$ in the denominator of (18), it follows that $\hat{\tau}^* < \tau^*$ whenever $\tau^* > 0$ (and $\hat{\tau}^* = 0$ when $\tau^* = 0$), thus the inequality in (20) holds whenever $\hat{\tau} \leq 2\hat{\tau}^*$. It follows, then, that $h_{\hat{\tau},ij}(\boldsymbol{z}) \leq h_{0,ij}(\boldsymbol{z})$ whenever $\hat{\tau} \leq 2\hat{\tau}^*$. □

**Remark 1.** *The condition $\hat{\tau} \leq 2\hat{\tau}^*$ may be satisfied $\forall \hat{\tau}^* \geq 0$ for choices of $k \geq 1$ in $K_\delta(t)$. Since $k$ is a shape parameter for the function $K$, higher values of $k$ lead to smaller approximation error $e_\tau = |\hat{\tau} - \tau^*|$ for $\tau^* \in [0, T]$. In practice, we use $k = 1000$.*

Since $h_{\hat{\tau},ij} \in \mathcal{C}^1$, we have by Definition 1 that if there exists a function $\alpha \in \mathcal{K}_\infty$ such that (4) holds then $h_{\hat{\tau},ij}$ is a valid CBF. Under such conditions, our ff-CBF may be synthesized with any nominal control law using (5) for communicating agents or (7) for non-communicating agents. In contrast to when used with a generic CBF, the decentralized control law (7) guarantees collision avoidance under our ff-CBF $h_{\hat{\tau},ij}$ and dynamics (8) (as long as it is feasible) provided that all vehicles deploy (7) with $h_{\hat{\tau},ij}$ and are not turning, i.e. $\psi_i = \beta_i = 0$. This is because $L_f h_{\hat{\tau},ij} \to 0$ as[2] $\hat{\tau} \to \tau^*$, in which case (7c) becomes

$$L_{g_i} h_{\hat{\tau},ij} \boldsymbol{u}_i + \alpha_{ij}(h_{\hat{\tau},ij}) \geq 0, \quad \forall i \in \mathcal{A}, \tag{21}$$

which, for any given two agent pair $i, j$ yields

$$\dot{h}_{\hat{\tau},ij} = L_{g_i} h_{\hat{\tau},ij} \boldsymbol{u}_i + L_{g_j} h_{\hat{\tau},ji} \boldsymbol{u}_j \geq -\alpha_{ij}(h_{\hat{\tau},ij}) - \alpha_{ji}(h_{\hat{\tau},ji})$$

where $h_{\hat{\tau},ij} = h_{\hat{\tau},ji}$, which satisfies (3) and thus prevents collisions. Intuitively, a zero CBF drift term i.e. $L_f h_{\hat{\tau},ij} = 0$ is explained by the fact that the ff-CBF $h_{\hat{\tau},ij}$ is already predicting the future minimum distance between vehicles $i$ and $j$ under zero-acceleration policies, thus in the absence of an acceleration input the prediction is correct and the minimum distance between vehicles is reached at time $t + \hat{\tau}$.

Note that the zero level set defined by candidate CBF $h_{\hat{\tau},ij}$ represents a *virtual* barrier. Specifically, $h_{\hat{\tau},ij}(\boldsymbol{z}_i, \boldsymbol{z}_j) < 0$ does not imply that a collision has occurred ($h_{0,ij}(\boldsymbol{z}_i, \boldsymbol{z}_j) < 0$), nor does it suggest that one is unavoidable; rather, $h_{\hat{\tau},ij}(\boldsymbol{z}_i, \boldsymbol{z}_j) < 0$ implies that a future collision will occur if the zero-acceleration control policy, $\hat{\boldsymbol{u}}_k$, is applied uniformly by each vehicle $k \in \{i, j\}$. This motivates the notion of the relaxed future-focused control barrier function (rff-CBF):

$$H_{ij}(\boldsymbol{z}_i, \boldsymbol{z}_j) = h_{\hat{\tau},ij}(\boldsymbol{z}_i, \boldsymbol{z}_j) + \alpha_0\left(h_{0,ij}(\boldsymbol{z}_i, \boldsymbol{z}_j)\right), \tag{22}$$

[2]In our simulations, we have found that $L_f h_{\hat{\tau},ij}$ is on the order of the approximation error $e_\tau = |\hat{\tau} - \tau^*| \approx 10^{-9}$ for $\tau^* \in [0, \bar{\tau}]$, which may be accounted for by subtracting $\varepsilon \approx 10^{-9}$ from the left-hand side of (21).

where $\alpha_0 \in \mathcal{K}_\infty$. The zero super-level set of $H_{ij}$ is then

$$\mathcal{S}_{H,ij} = \{(\boldsymbol{z}_i, \boldsymbol{z}_j) \in \mathbb{R}^{2n} \mid H_{ij}(\boldsymbol{z}_i, \boldsymbol{z}_j) \geq 0\}, \tag{23}$$

which defines a *relaxed* virtual barrier that allows virtual constraint violations away from the physical barrier, and in that sense enlarges the admissible control space while preserving the collision avoidance guarantee. This is proved in the following result.

**Theorem 2.** *Consider two agents, each of whose dynamics are described by (1). Suppose that $H_{ij}$ is given by (22), and that $H_{ij} \geq 0$ at $t = 0$. If there exist control inputs, $\boldsymbol{u}_i$ and $\boldsymbol{u}_j$, such that the following condition holds, for all $t \geq 0$,*

$$\sup_{\substack{\boldsymbol{u}_i \in \mathcal{U}_i \\ \boldsymbol{u}_j \in \mathcal{U}_j}} \left[L_{f_i} H_{ij} + L_{f_j} H_{ij} + L_{g_i} H_{ij} \boldsymbol{u}_i + L_{g_j} H_{ij} \boldsymbol{u}_j\right] \geq 0, \tag{24}$$

*for all $\boldsymbol{z} \in \partial\mathcal{S}_{H,ij}$, then, the physical safe set defined by $\mathcal{S}_{0,ij}(t) = \{(\boldsymbol{z}_i, \boldsymbol{z}_j) \in \mathbb{R}^{2n} \mid h_{0,ij}(\boldsymbol{z}_i, \boldsymbol{z}_j) \geq 0\}$ is forward-invariant under $\boldsymbol{u}_i$, $\boldsymbol{u}_j$, i.e. there is no collision between agents $i$ and $j$.*

*Proof.* In order to show that $\mathcal{S}_{0,ij}$ is rendered forward-invariant by (24), we must show that (24) implies that $\dot{h}_{0,ij} \geq 0$ whenever $h_{0,ij} = 0$. We will prove this by contradiction.

Suppose that $H_{ij}, h_{0,ij} = 0$, and that (24) holds but $\dot{h}_{0,ij} < 0$. Note also that by Theorem 1 $h_{\hat{\tau},ij} \leq h_{0,ij}$. Then, it follows that $\dot{h}_{0,ij} = 2(\xi_x\nu_x + \xi_y\nu_y) < 0$, which by (17) implies that $\hat{\tau} > 0$. With $\hat{\tau} > 0$, it follows that $h_{\hat{\tau},ij} < h_{0,ij} = 0$. However, we have assumed that $H_{ij}, h_{0,ij} = 0$, which means by definition that $h_{\hat{\tau},ij} = 0$. Thus, we have reached a contradiction. It follows, then, that (24) implies that $\dot{h}_{0,ij} \geq 0$ whenever $h_{0,ij} = 0$. As such, $\mathcal{S}_{0,ij}$ is rendered forward-invariant. □

As a result of Theorem 2, we can use (22) to encode safety in the context of a CBF-QP control scheme (5) or (7). In the ensuing section, we conduct a comparative study on the efficacy of the nominal (13), future-focused (16), and relaxed future-focused (22) CBFs across randomized trials of an automotive intersection crossing problem.

## V. Intersection Case Studies

In this section, we illustrate the use of our future-focused CBFs for collections of both communicating and non-communicating vehicles in the context of simulated and experimental trials of an unsignaled intersection scenario. We provide code and a selection of videos for both on Github[3].

### A. Centralized Control: Simulated Trials

In an empirical study on a simulated 4-vehicle unsignaled intersection scenario, we illustrate how using a rff-CBF to control communicating vehicles in a centralized manner improves intersection throughput with promising empirical results on safety and QP feasibility. We study the varying

[3]Link to Github repository: github.com/6lackmitchell/ffcbf-control

degrees of success of three different centralized controllers of the form (5) to solve Problem 1, namely to find

$$\boldsymbol{u}_i^* = [\omega_i^* \ a_i^*]^\top, \ \forall i = 1, \dots, A, \tag{25}$$

where the turning rate is

$$\omega_i^* = \min\left(\max(\omega_i^0, -\bar{\omega}), \bar{\omega}\right), \tag{26}$$

and the accelerations $a_1^*, \dots, a_p^*$ are computed via

$$[a_1^* \dots a_p^*]^\top = \underset{[a_1 \dots a_p]}{\arg\min} \frac{1}{2} \sum_{i=1}^{p} (a_i - a_i^0)^2 \tag{27a}$$

$$\text{s.t.} \quad \forall i, j = 1, \dots, A, \ j \neq i$$

$$Aa_i \leq b, \tag{27b}$$

$$\phi_i + \gamma_i a_i \geq 0, \tag{27c}$$

$$\phi_{ij} + \boldsymbol{\gamma}_{ij,[i]} a_i + \boldsymbol{\gamma}_{ij,[j]} a_j \geq 0, \tag{27d}$$

where $\omega_i^0$ and $a_i^0$ denote the nominal inputs computed using LQR (see Appendix I for a detailed explanation), (27b) encodes input constraints of the form $-\bar{a} \leq a_i \leq \bar{a}$, (27c) enforces both the road speed limit and requires that vehicles do not reverse, and (27d) is the collision avoidance condition, where $\phi$ and $\gamma$ are as in (6). Specifically, the controllers under examination are (25) with

i) 0-CBF: $h_{ij} = h_{0,ij}$ according to (13)
ii) ff-CBF: $h_{ij} = h_{\hat{\tau},ij}$ from (16)
iii) rff-CBF: $h_{ij} = H_{ij}$ via (22)

with $\alpha_0(h_{0,ij}) = k_0 h_{0,ij}$, where $k_0 = 0.1 \max(\hat{\tau} - 1, \varepsilon)$, $\varepsilon = 0.001$, the look-ahead horizon $\bar{\tau} = 5$s, and $\alpha_{ij}(h_{ij}) = 10 h_{ij}$, $\bar{\omega} = \pi/2$, and $\bar{a} = 9.81$ for all cases. We note that (25) is centralized in the sense that it is assumed that all states, $\boldsymbol{z}_i$, and nominal control inputs, $\boldsymbol{u}_i^0$, are known.

For each study, we performed $N = 1000$ trials of simulated trajectories of 4 vehicles approaching the intersection from different lanes, all of whose dynamics are described by (8), using the control scheme described by (25) and a timestep of $\Delta t = 0.01$s. At the beginning of each trial, the vehicles were assigned to a lane and their initial conditions were randomized via

$$d_i = d_0 + U(-\Delta_d, \Delta_d),$$
$$\mathcal{S}_i = s_0 + U(-\Delta_s, \Delta_s),$$

where $d_i$ denotes the initial distance of vehicle $i$ from the intersection, $\mathcal{S}_i$ its initial speed, and $U(a, b)$ a sample from the uniform random distribution between $a$ and $b$. We chose $d_0 = 12$m, $\Delta_d = 5$m, $s_0 = 6$m/s, and $\Delta_s = 3$m/s, and screened out initial conditions in violation of Assumption 1. For the speed limit, we chose $v_{max} = 10$m/s.

For performance evaluation, we introduce some metrics:

i) Success: $\frac{\text{Number of Successful Trials}}{\text{Number of Trials}}$,
ii) Feas.: $\frac{\text{Number of Trials in which QP is Always Feasible}}{\text{Number of Trials}}$,
iii) DLock: $\frac{\text{Number of Trials in which Vehicles become deadlocked}}{\text{Number of Trials}}$,
iv) Unsafe: $\frac{\text{Number of Trials Vehicles in which } h_{0,ij} < 0}{\text{Number of Trials}}$,

where a successful trial is characterized as one where all vehicles exit the intersection at their desired location, a deadlock is characterized as when all vehicles have stopped and remained stopped for 3 sec, and we define "Avg. Time" as the average time in which the final vehicle reached the intersection exit over all successful trials.

TABLE I: Controller Performance – All Proceed Straight

| CBF | Success | Feas. | DLock | Unsafe | Avg. Time |
|---|---|---|---|---|---|
| $h_{ij} = h_{0,ij}$ | 0.653 | 1 | 0.347 | 0 | 5.67 |
| $h_{ij} = h_{\hat{\tau},ij}$ | 1 | 1 | 0 | 0 | 3.45 |
| $h_{ij} = H_{ij}$ | 1 | 1 | 0 | 0 | 3.21 |

TABLE II: Controller Performance – One Left Turn

| CBF | Success | Feas. | DLock | Unsafe | Avg. Time |
|---|---|---|---|---|---|
| $h_{ij} = h_{0,ij}$ | 0.689 | 1 | 0.311 | 0 | 7.75 |
| $h_{ij} = h_{\hat{\tau},ij}$ | 0.963 | 0.963 | 0 | 0 | 5.33 |
| $h_{ij} = H_{ij}$ | 1 | 1 | 0 | 0 | 4.91 |

We examined the performance of each controller under two circumstances: 1) each vehicle seeks to proceed straight through the intersection without turning, and 2) three vehicles seek to proceed straight without turning and one seeks to make a left turn. The results for the 3 different controllers are compiled in Tables I and II respectively. Although the 0-CBF in a centralized QP-based control law is known to guarantee safety and QP feasibility under certain conditions [22], such a controller has no predictive power and is therefore prone to deadlocks. We illustrate such a deadlock in Figure 3a. The ff-CBF-based controller succeeded as long as it was feasible, offering a 39% reduction in average time over the 0-CBF in the straight scenario and an 31% time improvement in the turning scenario, but suffered from virtual constraint violations leading to QP infeasibility in the case of turning vehicles, one example of which is shown in Figure 3b. The rff-CBF controller enjoyed both the same empirical feasibility and safety as the 0-CBF design and improved the average success time to a similar extent as the ff-CBF, specifically by 43% and 36% for the straight and turning scenarios respectively. In addition, the rff-CBF control scheme achieved 100% feasibility even in the turning scenario, despite the constant velocity prediction model not taking a change of heading into account. We leave any theoretical guarantees of feasibility, however, to future work. The state, control, and rff-CBF trajectories for a turning trial are illustrated in Figures 4-6. It can be seen from Figure 5 that the control actions smoothly take action in advance of any dangerous scenario, and from Figure 6 that both $H_{ij}$ and $h_{0,ij}$ remain non-negative for all $i$, $j$.

### B. Decentralized Control: Rover Experiments

We further demonstrated the success of our decentralized rff-CBF-QP controller on a collection of AION R1 UGV rovers in an intersection scenario in the lab. Each of the 5 rovers was asked to proceed straight through the intersection while obeying a speed limit (encoded via (9)) and avoiding collisions with each other (using rff-CBF (22)). Modeling the rovers as bicycles (8), we used a controller of the form (7) to compute acceleration $a_i$ and angular rate $\omega_i$ inputs in order

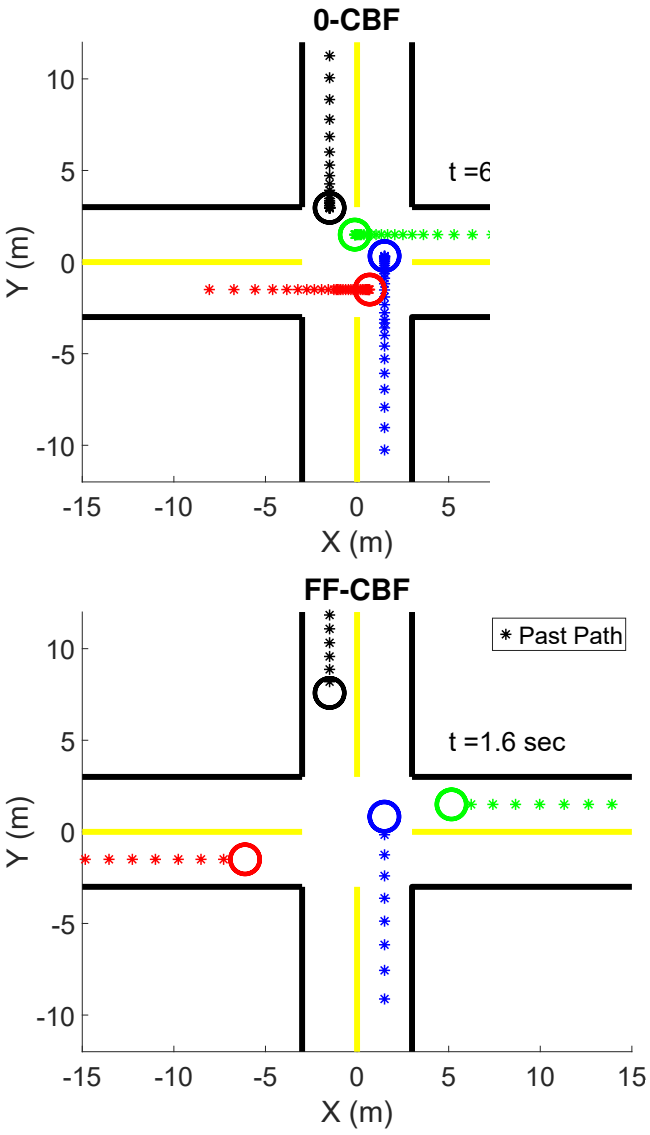


(b)

Fig. 3: Selected XY trajectories for the intersection crossing prob lem using (a) 0-CBF (Straight Trial 582) and (b) ff-CBF (Turnin Trial 137). In (a), the centralized controller has no predictive powe and the vehicles deadlock, whereas in (b) the virtual barrier betwee blue and black vehicles is violated despite a wide physical margi as the blue vehicle begins to turn left.

to send velocity $v_i(t_{k+1}) = v_i(t_k) + a_i \Delta t$ and $\omega_i$ command to the rovers' customized on-board PID controllers. The fu control loop ran at a frequency of 20Hz, where the nomina input $\boldsymbol{u}_0$ was computed using the LQR law outlined in Appendix I, position feedback was obtained using a Vicon motion capture system, the extended Kalman filter output from the PX4 firmware running via the on-board Pixhawk was used for state estimation.

As shown in Figure 7, our rff-CBF controller succeeds in driving the vehicles safely through the intersection without a deadlock. The video footage available at the above GitHub link shows that, contrary to behavior expected using traditionally myopic, present-focused CBFs, some rovers accelerated into the intersection in order to avoid predicted

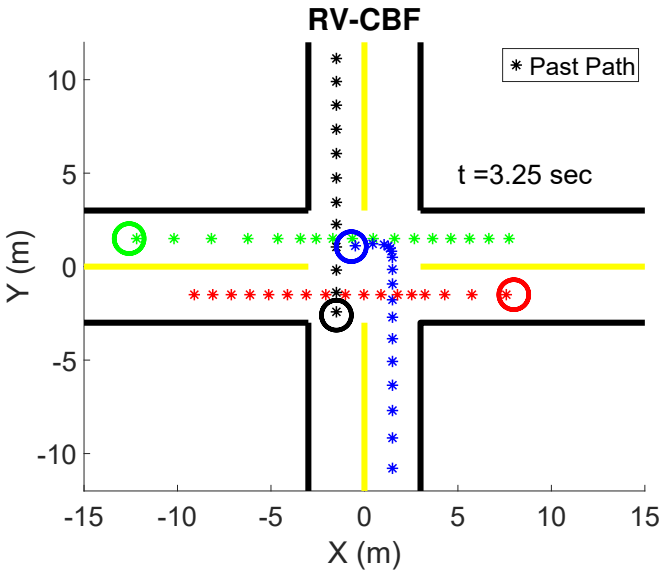


Fig. 4: XY trajectories for Trial 650 of the rff-CBF simulation set.

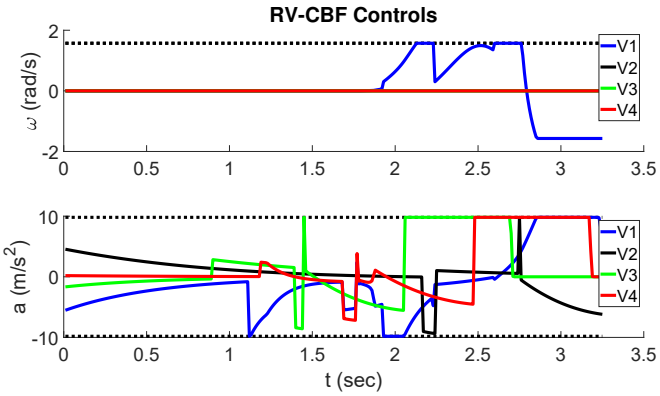


Fig. 5: Control solutions for Trial 650 of rff-CBF simulation set.

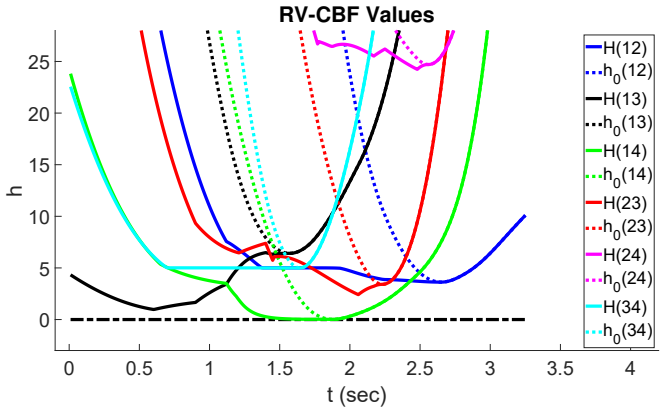


Fig. 6: rff-CBF ($H$) and 0-CBF ($h_0$) trajectories for rff-CBF Trial 650. $(ij)$ denote that CBF is evaluated for vehicles $i$ and $j$.

future collisions whereas others braked to await their turn.

## VI. Conclusion

In this paper, we introduced advancements to traditionally myopic CBF-based safe control in the form of novel future-focused (ff-) and relaxed future-focused (rff-) CBFs. We then studied their efficacy on a simulated intersection

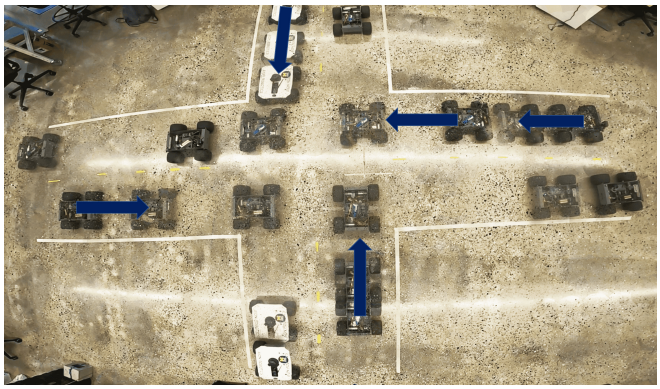

Fig. 7: Five rovers safely traverse a four-way intersection in the laboratory environment using a decentralized rff-CBF-QP control law. The rovers at their initial positions are marked with arrows pointing in the direction of motion.

crossing problem for a collection of automobiles modeled as bicycles and controlled by a centralized CBF-QP controller under three different CBFs. We discovered that the rff-CBF performed best in practice. We further validated our proposed approach on a collection of 5 ground rovers in an intersection scenario in the lab environment. In the future, we plan to further investigate 1) how rff-CBFs and control Lyapunov functions may be combined to make formal guarantees on stabilization and safety, and 2) under what conditions the nominal CBF-QP controller remains feasible when the future-focused CBF-QP may not be.

## References


[1] (2020, Sep) A new idc forecast shows how vehicles will gradually incorporate technologies that lead to autonomy. [Online]. Available: https://www.idc.com/getdoc.jsp?containerId=prUS46887020

[2] (2021, Aug) Office of research, development, and technology at the turner-fairbank highway research center: Intersection safety. [Online]. Available: https://highways.dot.gov/research/research-programs/safety/intersection-safety

[3] K. Dresner and P. Stone, "A multiagent approach to autonomous intersection management," *Journal of artificial intelligence research*, vol. 31, pp. 591–656, 2008.

[4] K. Yang, S. I. Guler, and M. Menendez, "Isolated intersection control for various levels of vehicle technology: Conventional, connected, and automated vehicles," *Transportation Research Part C: Emerging Tech.*, vol. 72, pp. 109–129, 2016.

[5] M. Khayatian, Y. Lou, M. Mehrabian, and A. Shirvastava, "Cross-roads+ a time-aware approach for intersection management of connected autonomous vehicles," *ACM Transactions on Cyber-Physical Systems*, vol. 4, no. 2, pp. 1–28, 2019.

[6] A. D. Ames, X. Xu, J. W. Grizzle, and P. Tabuada, "Control barrier function based quadratic programs for safety critical systems," *IEEE Trans. on Automatic Control*, vol. 62, no. 8, pp. 3861–3876, 2017.

[7] W. Xiao, C. Belta, and C. G. Cassandras, "Decentralized merging control in traffic networks: A control barrier function approach," in *Proceedings of the 10th ACM/IEEE International Conf. on Cyber-Physical Systems*, New York, NY, USA, 2019, p. 270–279.

[8] M. Black, K. Garg, and D. Panagou, "A quadratic program based control synthesis under spatiotemporal constraints and non-vanishing disturbances," *59th IEEE Conf. on Decision and Control*, 2020.

[9] M. Rauscher, M. Kimmel, and S. Hirche, "Constrained robot control using control barrier functions," in *IEEE/RSJ International Conference on Intelligent Robots and Systems*, 2016, pp. 279–285.

[10] L. Wang, E. A. Theodorou, and M. Egerstedt, "Safe learning of quadrotor dynamics using barrier certificates," in *2018 IEEE International Conf. on Robotics and Automation*, 2018, pp. 2460–2465.

[11] M. Jankovic, "Robust control barrier functions for constrained stabilization of nonlinear systems," *Automatica*, vol. 96, pp. 359–367, 2018.

[12] M. Black, E. Arabi, and D. Panagou, "A fixed-time stable adaptation law for safety-critical control under parametric uncertainty," in *2021 European Control Conference (ECC)*, 2021, pp. 1328–1333.

[13] J. Zeng, B. Zhang, and K. Sreenath, "Safety-critical model predictive control with discrete-time control barrier function," in *2021 American Control Conference (ACC)*, 2021, pp. 3882–3889.

[14] R. A. Freeman and P. V. Kokotovic, "Inverse optimality in robust stabilization," *SIAM Journal on Control and Optimization*, vol. 34, no. 4, pp. 1365–1391, 1996.

[15] F. Castaneda, J. J. Choi, B. Zhang, C. J. Tomlin, and K. Sreenath, "Gaussian process-based min-norm stabilizing controller for control-affine systems with uncertain input effects and dynamics," in *2021 American Control Conference (ACC)*. IEEE, 2021, pp. 3683–3690.

[16] H. Yuqing and H. Jianda, "Generalized point wise min-norm control based on control lyapunov functions," in *2007 Chinese Control Conference*. IEEE, 2007, pp. 404–408.

[17] J. Breeden and D. Panagou, "Predictive control barrier functions for online safety critical control," *arXiv preprint arXiv:2204:00208*, 2022.

[18] T. Gurriet, M. Mote, A. Singletary, P. Nilsson, E. Feron, and A. D. Ames, "A scalable safety critical control framework for nonlinear systems," *IEEE Access*, vol. 8, pp. 187 249–187 275, 2020.

[19] Y. Chen, M. Jankovic, M. Santillo, and A. D. Ames, "Backup control barrier functions: Formulation and comparative study," *arXiv preprint arXiv:2104.11332*, 2021.

[20] A. Singletary, A. Swann, Y. Chen, and A. D. Ames, "Onboard safety guarantees for racing drones: High-speed geofencing with control barrier functions," *IEEE Robotics and Automation Letters*, vol. 7, no. 2, pp. 2897–2904, 2022.

[21] F. Blanchini, "Set invariance in control," *Automatica*, vol. 35, no. 11, pp. 1747–1767, 1999.

[22] M. Jankovic and M. Santillo, "Collision avoidance and liveness of multi-agent systems with cbf-based controllers," in *2021 60th IEEE Conference on Decision and Control (CDC)*, 2021, pp. 6822–6828.

[23] R. Rajamani, *Vehicle Dynamics and Control*. Springer US, 2012.

[24] J. Kong, M. Pfeiffer, G. Schildbach, and F. Borrelli, "Kinematic and dynamic vehicle models for autonomous driving control design," in *2015 IEEE Intelligent Vehicles Symposium (IV)*, 2015, pp. 1094–1099.

[25] M. Santillo and M. Jankovic, "Collision free navigation with interacting, non-communicating obstacles," in *2021 American Control Conference (ACC)*, 2021, pp. 1637–1643.


## Appendix I
## LQR-based Nominal Control Law

For each vehicle, we assume that a desired state trajectory, $\boldsymbol{q}_i^*(t) = [x_i^* \;\; y_i^* \;\; \dot{x}_i^* \;\; \dot{y}_i^*]^\top$, is available. Then, we define the modified state vector and tracking error as $\boldsymbol{\zeta}_i(t) = [x_i \;\; y_i \;\; \dot{x}_i \;\; \dot{y}_i]^\top$, and $\tilde{\boldsymbol{\zeta}}_i(t) = \boldsymbol{\zeta}_i(t) - \boldsymbol{q}_i^*(t)$ respectively. We then compute the optimal LQR gain, $K$, for a planar double integrator model and compute $\boldsymbol{\mu} = [a_{x,i} \;\; a_{y,i}]^\top = -K\tilde{\boldsymbol{\zeta}}_i$. Then, we map $a_{x,i}$, $a_{y,i}$ to $\omega_i^0$, $a_i^0$ via

$$\begin{bmatrix} \omega_i^0 \\ a_i^0 \end{bmatrix} = S^{-1} \begin{bmatrix} a_{x,i} + \dot{y}_i\dot{\psi}_i \\ a_{y,i} - \dot{x}_i\dot{\psi}_i \end{bmatrix},$$

where

$$S = \begin{bmatrix} -v_i \sin(\psi_i)\sec^2(\beta_i) & \cos(\psi_i) - \sin(\psi_i)\tan(\beta_i) \\ v_i \cos(\psi_i)\sec^2(\beta_i) & \sin(\psi_i) + \cos(\psi_i)\tan(\beta_i) \end{bmatrix},$$

the inverse of which exists as long as $v_i \neq 0$. Therefore, if $|v_i| < \epsilon$, where $0 < \epsilon \ll 1$, we assign $\omega_i^0 = 0$ and $a_i^0 = \sqrt{a_{x,i}^2 + a_{y,i}^2}$.